The Role of Defect Microstructure in the Crystallization Behavior of Metallocene and $MgCl_2$-Supported Ziegler-Natta Isotactic Poly(Propylenes)

Rufina G. Alamo
Florida Agricultural and Mechanical University and Florida State University College of Engineering, Departament of Chemical Engineering, USA

Abstract: The intermolecular defect distribution of poly(propylenes) of the Ziegler-Natta (ZN) and metallocene (M) types is assessed by classical fractionation and analysis of the fractions by GPC and ^{13}C NMR. In addition, the linear growth rates, a property sensitive to differences in defects distribution in the poly(propylene) chain, are used to infer the stereoblock-like intramolecular distribution of defects in industrial type ZN iPPs and their fractions. The behavior of fractions from a matched metallocene iPP provide direct evidence of the single-site nature of the catalyst.
Metallocene poly(propylenes) enable a quantitative assessment of the molecular, thermodynamic and kinetic factors that govern the formation and concentrations of the α and γ polymorphs. Short continuous crystallizable sequences and high crystallization temperatures favor the formation of this polymorph in homo poly(propylenes) and random propylene copolymers. Differences in the partitioning of the comonomer between the crystalline and non-crystalline regions leads to contents of the gamma phase that differ among the copolymers at any given crystallization temperature. Qualitatively these differences can be used to assess the degree to which a counit participates in the crystallite.

Keywords: *Metallocene, Ziegler-Nata, crystallization, polypropylenes.*

Introduction

Semicrystalline polymers offer the highly desirable combination of strength conferred by crystalline arrays and toughness provided by finely dispersed non-crystalline regions. The morphology and orientation distribution of this spontaneously formed, nano-scale composite structure dictates the ultimate material properties. Semicrystalline polyolefins enable the production of high strength fibers and films, and a diversity of extruded and injection molded parts used in household, automotive, microelectronics and biomedical industries playing a vital role in economic growth. Yet fundamental understanding of the role of molecular structure in the evolving morphology through the various processes remains unknown. Novel metallocene type catalysts allow control of molecular structure in ways unprecedented and not feasible in polymerizations with catalysts of the Ziegler-Natta type. They enable control structures for a better characterization and prediction of key components in the evolution of ordered structures during solidification of the ZN products, still produced in very high volumes.

The influence of the type of catalyst and polymerization process on microstructures of industrial ZN poly(propylene)s has been classically studied by fractionation and ^{13}C NMR analysis of the fractions[1, 2]. However, the generality of the distribution of defects has been hampered because, historically, ZN catalysts have been modified to increase the isotacticity level. Coupled to these modifications is a possible change in the mechanism that dictates stereospecificity and a reduced sensitivity in the spectroscopic detection of stereosequences. Consequently, the influence of a catalyst in the defect microstructure is often reevaluated as higher field NMR spectrometers, with higher resolution and sensitivity, become available[3-10]. TREF[2,11] and solvent gradient extraction[12] have led to fractions of increasing isotacticity and increasing molar mass, a result that clearly indicates a non uniform inter chain composition of defects, otherwise then expected from the inferred multiplicity of sites.

The question that is most difficult to address by analysis of the NMR spectra or from the fractionation results is the nature of the intramolecular defect distribution, i.e. if the defects within a given chain deviate strongly from the random distribution. To address this issue some investigators have fitted the experimental stereosequences with statistical models[7,10]. Along these lines, it was also observed that most of the fractions contained syndiotactic *rrrr* pentads[4,7-10,13,14] and it was proposed that some of the propagation errors were "blocky" in nature. Thus, the presence of stereoblocks in the ZN-iPP has been inferred or suspected by most previous investigators and emphasized in Busico et al.'s latest work[13]. A drawback in any of the ^{13}C NMR stereosequence analysis or fittings, is that the experimental NMR data comes from very short sequences (up to a nonad distribution). Thus stereodefects that terminate continuous isotactic sequences

***Autor para correspondência: Rufina G. Alamo**, Florida Agricultural and Mechanical University and Florida State University College of Engineering. Department of Chemical Engineering. Tallahassee, FL 32310. USA. E-mail:*

of 10 units or 1,000 units are indistinguishable. Consequently, any inference of a non-random intramolecular distribution of stereodefects must be obtained from the properties of the polypropylene fractions[15]. These indirect analyses are missing in the majority of earlier works dealing with elucidating distributions of stereo defects in ZN polypropylenes. The crystallization rates, a property highly sensitive to defects distribution, is now used to infer the intramolecular distribution of defects in the ZN iPP molecules. Moreover, the behavior of fractions from the metallocene iPP provided direct evidence of the uniform interchain distribution of defects and the single site nature of the catalyst[15].

The concentration of stereo defects, regio defects, or comonomers randomly inserted in the poly(propylene) chain can now be controlled using metallocene catalysts. Thus, properties of iPPs can be studied as a function of the type and the fractional content of these defects for a fixed molecular weight and molecular weight distribution. One of the properties that is greatly affected by content and distribution of defects is the formation of the gamma or orthorhombic polymorph. As the concentration of defects in industrial iPPs will be increased as a mean to change properties, for example, reduce crystallinity, lower the softening point and improve impact properties and processability, the details of structural and kinetic factors that control the formation of this polymorph become of practical interest and beyond a pure scientific curiosity.

Previous detailed studies of homopolymers have found a close correlation between the concentration and distribution of these irregularities and the maximum content of gamma polymorph that the chain develops[16]. While molecular mass (in a range of 40,000 – 300,000 g/mol) has only a minor effect on the formation of the gamma polymorph, the concentration of defects has a major effect, increasing the content of this polymorph. The studies in homopolymers were expanded to include the effect of comonomers of the 1-alkene type in the formation of the gamma phase and to determine in what extent the type of comonomer influences the crystallographic polymorphs[17]. The most relevant results coupled with the spherulitic and lamellar structures characteristic of each polymorph is presented here.

Defects Distributions

From a crystallization perspective, the defects of the polypropylene chain confer a copolymeric character to the molecule. Theoretical accounts of the crystallization and melting of these "copolymers" have been undertaken from phase equilibrium consideration involving more than one species[18]. When defects are rejected from the crystal, the equilibrium melting/crystallization temperature does not depend directly on the composition of the copolymer but rather upon the sequence distribution of crystallizable sequences. The sequence distribution probability (p) of a block copolymer is one. This requires that there is no depression in the melting or crystallization of block copolymers with increasing lengths or numbers of blocks. The unchanged undercooling leads to constant crystallization rates. Conversely, the parameter p of a

Table 1. Characterization of parent polymers and fractions from Metallocene and ZN-iPP

Sample	Mw (g/mol)	Mw/Mn	Stereo defects (mol%)	Regio defects (mol%)	Total defects (mol%)	Tm (°C)[a]	ΔH (J/g)[a]
M203K0.51 Parent	203,900	2.00	0.11	0.40	0.51	155.0	76.0
Mf 86K0.56	86,000	1.43	0.16	0.40	0.56	156.2	85.7
Mf 121K0.50	121,000	1.32	0.11	0.39	0.50	156.3	75.2
Mf 143K0.54	143,000	1.24	0.07	0.47	0.54	156.1	86.0
Mf 200K0.46	200,000	1.23	0.08	0.38	0.46	155.8	80.4
Mf 235K0.45	235,000	1.24	0.07	0.38	0.45	154.6	93.1
Mf 358K0.41	358,000	1.34	0.07	0.34	0.41	154.0	73.5
Mf 383K0.41	383,000	1.47	na[b]	na	na	na	
Z263K0.51 parent	262,600	3.19	0.51	—	0.51	161.4	79.4
Zf 97K1.03	97,000	1.31	1.03	—	1.03	159.0	89.6
Zf 163Kxxx	157,000	1.27	Na	—	na	na	
Zf 163K0.60	163,000	1.97	0.60	—	0.60	161.3	80.5
Zf 204K0.41	204,000	2.15	0.41	—	0.41	160.9	81.6
Zf 328K0.36	328,000	1.77	0.36	—	0.36	162.3	81.5

[a]Rapidly quenched samples to 25 ºC. Tm: Peak melting temperature, ΔH: Heat of fusion
[b]Data not available.

random copolymer is less than one and, on equilibrium considerations, melting or crystallization are largely depressed with increasing concentration of defects in the chain. The change in undercooling affects the crystallization kinetics of these copolymers accordingly. These theoretical accounts give the basis for a comparative discussion of the crystallization behavior of fractions from a ZN iPP and those from a metallocene one in regards to their defect microstructure. In addition to the inferred intermolecular distribution by TREF, GPC and NMR data of ZN iPP fractions, their adherence to or deviation from the behavior of a matched metallocene iPP can probe the intramolecular defect distribution of the ZN iPP fractions.

A fractionation by molecular mass via supercritical fluid extraction in n-propane of matched Zn iPP and M iPP (same Mw and average concentration of defects), led to fractions with the characteristics listed in Table 1[15]. The concentration of defects of the metallocene fractions is basically constant within the series, providing direct evidence of the narrow interchain composition distribution of the parent M-iPP. However, as the molar mass of the ZN-iPP fractions increase, the defect concentration decreases from 1.03 to 0.36 mol% respectively, evidencing the expected inter-chain heterogeneity of defect distribution in the parent ZN iPP, also observed in other studies[1, 2,11]. It is apparent that the ZN iPP contains a fraction of highly isotactic long molecules which are not present in the metallocene iPP. This structural difference explains the ~8 °C higher melting temperature of the parent ZN iPP and increased growth rates compared to those of the M iPP. Longer isotactic sequences found in the ZN-iPP are selected earlier during crystallization and lead to a fraction of thicker crystallites that melt at higher temperatures than the crystals formed from the M-iPP with more uniformly distributed defects. In contrast, and as a consequence of differences in nucleation density, the overall crystallization rates of M iPP were found faster than those of the ZN iPP and do not correlate with the defect microstructure of the molecule. The fractionation results alone do not allow conclusions about the nature of the intramolecular defect distribution. This issue can only be inferred after analysis of the properties of the individual fractions.

The spherulitic linear growth rates of the metallocene fractions and the ZN fractions are shown in Figure 1a and 1b respectively. Both series display the classical strong negative temperature coefficient dictated by nucleation and growth theories. In addition, the growth rates of the metallocene fractions show a small but systematic decrease with molecular mass, following the pattern of other homopolymers and copolymers[19-21]. The increased number of entanglements per chain in the melt is clearly reflected in a reduced segmental transport to the crystallite site during the crystallization process.

Metallocene iPPs with total defect content increasing from 0.3 to 2.35 mol% allow the evaluation of the effect of increasing concentration of defects on the growth rates. The experimental data are given in Figure 2. The growth rate decreases about two orders of magnitude when the total defect content is increased in the range studied. An increase in non-crystallizable structural irregularities leads to a reduction of the amount of crystallizable sequences and, thus, to a decrease in the crystallization rate. This behavior is analogous to the overall crystallization rates of a series of random ethylene copolymers.

In contrast to the behavior of M-iPP fractions, the growth rates of the ZN-iPP fractions, shown in Figure 1b, do not display any systematic variation of G with either molar mass or concentration of defects. Should the defects in each ZN fraction be randomly distributed, one would have expected a significantly lower G for the fraction with 1.03 mol% defects, as indicated by the behavior of metallocene iPPs in Figure 2.

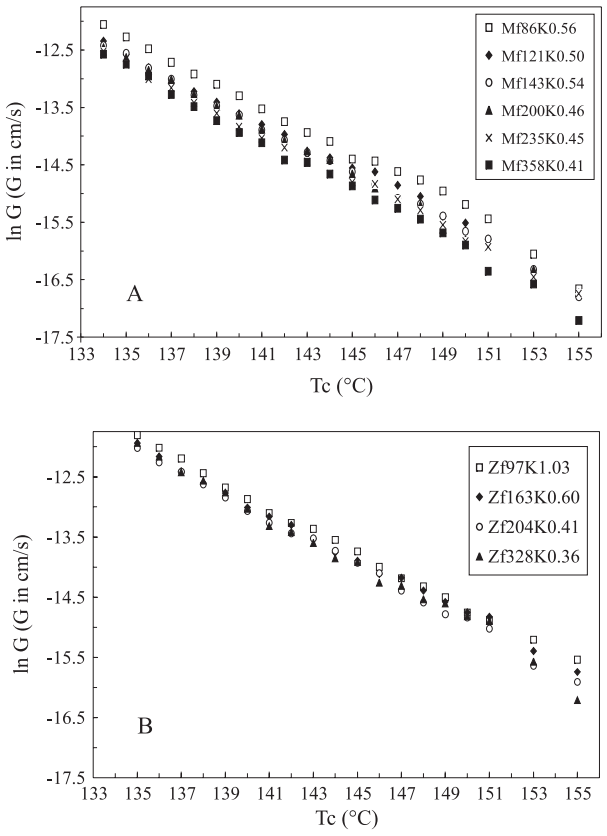

Figure 1. Linear growth rates of molecular mass fractions of (a) ZN iPP and (b) M iPPas function of Tc.

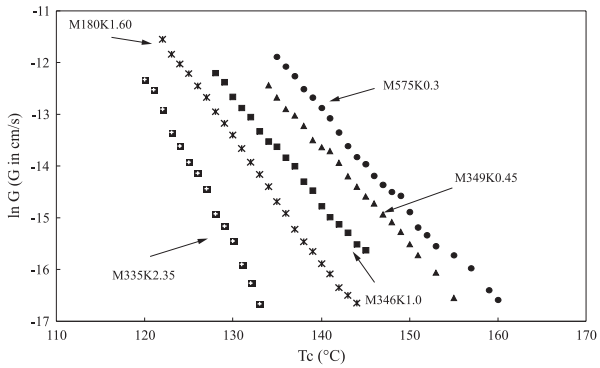

Figure 2. Linear growth rates of M iPPs with different concentration of defects.

Furthermore, there are only minor differences between the growth rates of any ZN-iPP fraction at a fixed crystallization temperature. The invariance of the linear growth rates among the ZN fractions, even after correction for differences in the molecular mass, is consistent with a stereo blocky intramolecular distribution of defects in all ZN-iPP molecules. This result is supported by the significantly lower contents of gamma polymorph that ZN iPP fractions develop compared to metallocene iPPs with matched concentrations of defects.

The proposed schematic model of defects distribution in the parent Zn iPP that conforms to the observed growth rates and polymorphic behavior is shown in Figure 3. In this model, the intermolecular defect composition is non-uniform with the shorter chains having a higher concentration of non isotactic units so as to comply with the fractionation behavior. However, the intramolecular distribution of defects is blocky. All chains display similar types of long crystallizable sequences, which are highlighted in the schematic figure. Following theoretical expectations, molecular fractions from this model show negligible differences in crystallization rates.

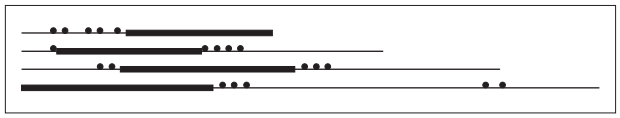

Figure 3. Model for stereosequence distribution in parent ZN iPP.

Crystallographic Polymorphs

Isotactic poly(propylene) exhibits three different crystallographic polymorphs, all with the classical 3_1 helix chain conformation. The difference between the polymorphs is the manner in which the chains are packed in the unit cell. Most iPPs rapidly crystallized from the melt develop the monoclinic or α form. The lamellar morphology associated with this polymorph is unusual. In addition to radially oriented lamellae, transverse lamellae grow tangentially to primary ones leading to the so-called crosshatched morphology[22-24]. The β or hexagonal form is usually obtained by adding specific nucleating agents. The chain packing in the unit cell of the γ form is orthorhombic and unique for polymeric systems in that the chain axes are non-parallel to one another. In the γ phase successive bilayers of parallel chains with opposite hand helices are tilted at 81° with respect to each other.

The structural, thermodynamic and kinetic factors governing the formation and concentration of the α and γ polymorphs in a series of metallocene catalyzed isotactic poly(propylenes) have been studied in detail[16]. The results of the homopolymers enable a quantitative framework within which the underlying bases that lead to the formation of the γ polymorph were discussed. The concentration of the γ phase is favored with increasing concentration of defects. Increasing crystallization temperature (Tcrys) also favored the formation of this polymorph up to a maximum value. With further increase of Tcrys the content of the gamma phase decreases[16]. While the increase of the maximum of the γ content with increasing concentration of defects is associated with a decreasing average length of continuous isotactic sequences, the maximum observed with increasing Tcrys points to an interplay of two competing processes. On one hand, packing energy calculation suggest that the γ form would be slightly more stable than the α phase[25]. Hence, it is thermodynamically more stable than the α phase and favored with increasing Tcrys. On the other hand, the concentration of short sequences available for crystallization decreases with increasing Tcrys. The result is a maximum in the concentration of the gamma form with Tcrys. The maximum has been confirmed in other studies with similar metallocene-based iPPs[26].

Contrasting with the random defect distribution of metallocene-based iPPs, those prepared with ZN catalysts (or their fractions) exhibit a stereoblock defect distribution and lead, for a matched average defect concentration, to much longer crystallizable sequences. Consequently, the content of gamma phase developed by ZN iPPs is significantly reduced[15, 16, 27].

The irregularities conferred by the comonomers to the poly(propylene) chain affect the formation of the γ polymorph in a manner akin to that given by stereo and regio defects. An example is given in Figure 4 for a series of metallocene propylene-ethylene copolymers with ethylene content ranging from 0.8 to 7.5 mol% (or from 1.8 to 8.7 mol% when stereo and regio defects, also present in the chain, are added to the comonomer content)[17]. A local maximum in the gamma content with Tcrys is also observed for the copolymer with the lowest defect concentration. It is not developed in the rest of the copolymers studied due to the unduly long

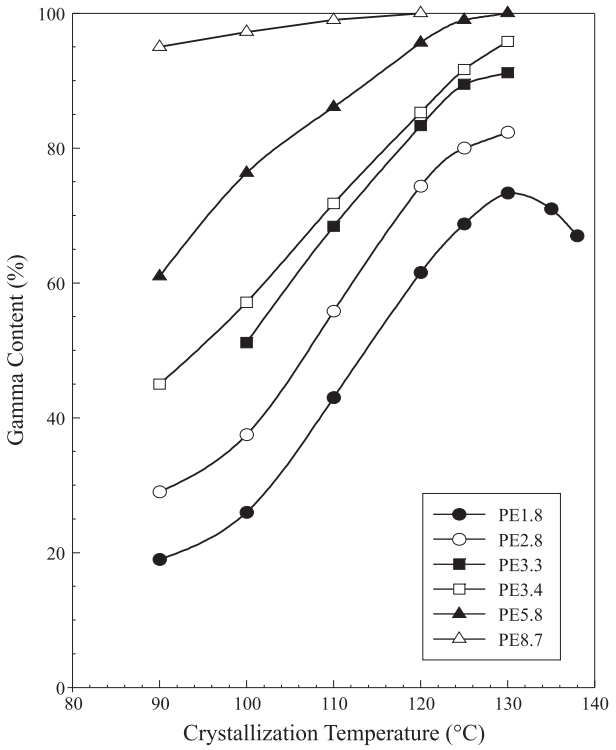

Figure 4. Percentage of γ phase as a function of crystallization temperature for propylene ethylene copolymers with ethylene content increasing from 0.8 to 7.5 mol%

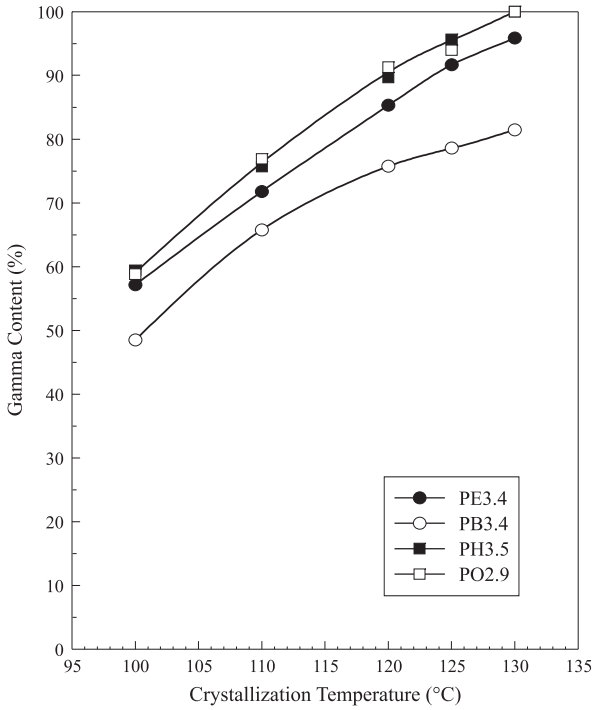

Figure 5. Percentage of γ phase as a function of crystallization temperature for propylene copolymers with ~ 3.3 mol% defects.

crystallization kinetics at Tcrys above 130 °C and depletion of long crystallizable sequences for the highest defected copolymers. Thus, these copolymers crystallize exclusively in the γ phase for Tcrys > 120 °C.

Similar results were obtained in a series of propylene 1-butenes, propylene 1-hexenes and propylene 1-octenes[17]. However, when the γ content is compared for the four types of copolymers, all with the same total defect concentration (~ 3.3 mol%), significant differences between them are found as seen in Figure 5. The 1-butene units lead to the lowest concentration of γ followed by the ethylene units. The data for the propylene 1-hexene and propylene 1-octene share a common curve and have the highest concentration of the γ phase with values ranging from ~60 to 100 % with increasing Tcrys. These differences are consistent with a different ability of cocrystallization of each type of comonomer with the propylene units. Ethylene and 1-butene units are partially accommodated in the crystalline regions while the 1-hexene and 1-octene units are preferentially rejected[28, 29]. With a higher probability of 1-butene units to enter the crystalline lattice[29], at the same total concentration of defects, its average crystallizable sequence length is the longest of the four copolymers investigated and may account for the observed higher melting temperatures[17,30]. The results of Figure 5 are important because they enable a quantitative framework to assess the degree to which a counit participates in the crystalline region.

As the concentration of the γ polymorph increases with increasing comonomer content or increasing crystallization temperature, a distinct lamellar morphology evolves. Long radially grown lamellae and branches hereon are replaced with short, transverse and regularly stacked lamellae. Examples for

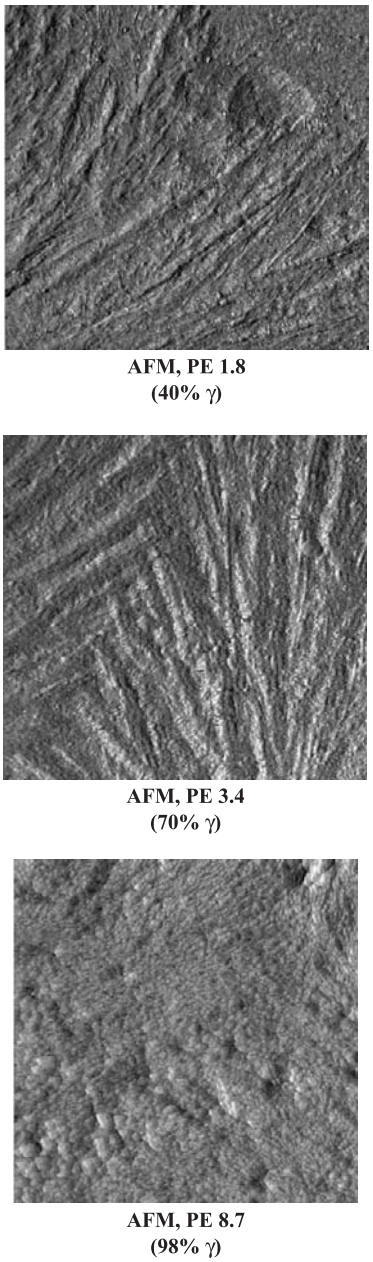

Figure 6. AFM 10 x 10 μm phase images of metallocene propylene ethylene copolymers. The total defect content and content of γ polymorph is indicated.

propylene ethylenes with increasing ethylene content, crystallized at 110 ºC are given in Figure 6. Spherulites are formed in copolymers with non-crystallizable units (1-hexene and 1-octene) up to ~ 3 mol% total defects and were observed up to ~6 mol% in those with partially crystallizable comonomers (ethylene and 1-butene)[31]. The ability to order short crystallizable sequences in the γ polymorph allows propagating lamellar-type crystallites in poly(propylenes) up to a high concentration of defects (~ 10 mol%).

Acknowledgements

Support of this work by the National Science Foundation (DMR-0094485) is gratefully acknowledged. Contributions to

this work by J.C. Randall, J.A. Blanco, S. Putcha, C. Chi, P.K. Agarwal, C.J. Ruff, E. Ritchson and D. Li are also acknowledged.

References

1. Paukkeri, R.; Vaananen, T.; Lehtinen, A. - *Polymer*, *34*, 2488 (1993).

2. Morini, G.; Albizzati, E.; Balbontin, G.; Mingizzi, I.; Sacchi, M. C.; Forlini, F.; Tritto, I. - *Macromolecules*, *29*, 5770 (1996).

3. Zambelli, A.; Locatelli, P.; Bajo, G.; Bovey, F. A. - *Macromolecules*, *8*, 687 (1975).

4. Zambelli, A.; Locatelli, P.; Provasoli, A.; Ferro, D. R. - *Macromolecules*, *13*, 267 (1980).

5. Kawamura, H.; Hayashi, T.; Inoue, Y.; Chujo, R. - *Macromolecules*, *22*, 2181 (1989).

6. Busico, V.; Corradini, P.; De Martino,L.; Graziano, F.; Iadicicco, A. M. - *Makromal. Chem.*, 192, 49 (1991).

7. Busico, V.; Corradini, P.; De Biasio, R.; Landriani, L.; Segre, A. L.; *Macromolecules*, *27*, 4521 (1994).

8. Busico, V.; Cipullo, R.; Corradini, P.; Landriani, L.; Vacatello, M. - *Macromolecules*, *28*, 1887 (1995).

9. Busico, V.; Cipullo, R.; Talarico, G.; Segre, A. L.; Chadwick, J. C. - *Macromolecules*, *30*, 4786 (1997).

10. Randall, J. C. - *Macromolecules 30*, 803 (1997).

11. Viville, P.; Daoust, D.; Jonas, A. M.; Nysten, B.; Legras, R.; Dupire, M.; Michel, J.; Debras, G. - *Polymer*, *42*, 1953 (2001).

12. Lehtinen, A.; Paukkeri, R. - *Macromol. Chem. Phys.*, *195*, 1539 (1994).

13. Busico, V.; Cipullo, R.; Monaco, G.; Talarico, G.; Vacatello, M.; Chadwick, J. C.; Segre, A. L.; Sudmeijer, O. - *Macromolecules*, *32*, 4173 (1999).

14. Chadwick, J. C.; Miedema, A.; Ruiseh, B. J.; Sudmeijer, O. - *Makromol. Chem., 193*, 1463 (1992).

15. Alamo, R. G.; Blanco, J. A.; Agarwal, P. K.; Randall, J. C. - *Macromolecules*, *36*, 1559 (2003).

16. Alamo, R. G.; Kim, M. H.; Galante, M. J.; Isasi, J. R.; Mandelkern, L. - *Macromolecules*, *32*, 4050 (1999).

17. Hosier, I. L.; Alamo, R. G.; Esteso, P.; Isasi, J. R.; Mandelkern, L. - *Macromolecules*, 36, 5623 (2003).

18. Flory, P. J. - *Trans. Faraday Soc.*, *51*, 848 (1955).

19. Ergoz, E.; Fatou, J. G.; Mandelkern, L. - *Macromolecules*, *5*, 147 (1972).

20. Alamo, R. G.; Mandelkern, L. - *Macromolecules*, *24*, 6480 (1991).

21. Lopez, L. C.; Wilkes, L. C. - *Polymer*, *29*, 106 (1988).

22. Brückner, S.; Meille, S. U.; Petraccone, U.; Pirozzi, B. - *Prog. Polym. Sci.*, *16*, 361 (1991).

23. Lotz, B.; Wittman, J. C.; Lovinger, A. J. - *Polymer*, *37*, 4979 (1996).

24. Padden, F. J.; Keith, H. D. - *J. Appl. Phys.*, *30*, 1479 (1959).

25. Ferro, D. R.; Brückner, S.; Meille, S. V.; Ragazzi, M. - *Macromolecules*, *25*, 5231 (1992).

26. De Rosa, C.; Auriemma, F.; Circelli, T.; Waymouth, R. M. - *Macromolecules*, *35*, 3622 (2002).

27. van der Burgt, F. P. T. J.; Rastogi, S.; Chadwick, J. C.; Rieger, B. - *J. Macromol. Sci. Phys.*, *B41*, 1091 (2002).

28. Alamo, R. G.; Vanderhart, D. L.; Nyden, M. R.; Mandelkern, L. - *Macromolecules*, *33*, 6094 (2000).

29. VanderHart, D. L.; Nyden, W. R.; Alamo, R. G.; Mandelkern, L. - *Polym. Prep.*, *82*, 140 (2000).

30. Hosoda, S.; Hori, H.; Yada, K.; Nakahara, S.; Tsuji, M. - *Polymer*, *43*, 7451 (2002).

31. Hosier, I. L.; Alamo, R. G.; Lin, J. S. (in progress)